Journal of the Serbian Chemical Society
JSCS-info@shd.org.rs • www.shd.org.rs/JSCS
J. Serb. Chem. Soc. *86* (3) 283–297 (2021)
JSCS–5421
Original scientific paper

Density functional theory calculation of propane cracking mechanism over chromium (III) oxide by cluster approach

TOYESE OYEGOKE[1,2]*, FADIMATU NYAKO DABAI[1], ADAMU UZAIRU[3] and BABA EL-YAKUBU JIBRIL[1]

[1]*Chemical Engineering Department, Faculty of Engineering, ABU Zaria, Nigeria,* [2]*Laboratoire de Chimie, ENS Lyon, l'Universite de Lyon, 69007, Lyon, France and* [3]*Chemistry Department, Faculty of Physical Sciences, ABU Zaria, Nigeria*

(Received 21 May, revised 18 July, accepted 20 July 2020)

Abstract: The catalyst coking and production of undesired products during the transformation of propane into propylene have been the critical challenges in the on purpose approach of propylene production. The mechanism contributing to this challenge was theoretically investigated through the analysis of cracking reaction routes. The study carried out employed the use of a density functional theory and cluster approach in order to understand the reactions that promote coking of the catalyst and in the search for the kinetic and thermodynamic data of the reaction mechanism involved in the process over Cr_2O_3. The rate-determining step and feasible route that easily promote the production of small hydrocarbons like ethylene, methane, and many others were identified. The study suggests Cr-site substitution or co-feeding of oxygen can aid in preventing deep dehydrogenation in the conversion of propane to propylene. This information will help in improving the Cr_2O_3 catalyst performance and further increase the production yield.

Keywords: catalyst deactivation; olefins; rate-determining step; scission; first principle; coking.

INTRODUCTION

Light alkenes, such as ethylene and especially propylene, are among the essential feedstock or precursors for petrochemical industries, and their global demand (utilization) is increasing day after day.[1] Dehydrogenation involves the transformation of materials like alkanes, which are of low-value, to alkenes (or olefins), which are commonly known for being highly reactive and valuable; examples of the elementary reactions involved in the process includes hydrogen abstraction (that is, propane to propylene) and cracking (that is, propane into lighter hydrocarbons like ethylene). Products like ethylene and propylene do

* Corresponding author. E-mail: ToyeseOyegoke@gmail.com, Toyese.Oyegoke@ens-lyon.fr
https://doi.org/10.2298/JSC200521044O

serve as precursors to the production of aldehydes, alcohols, aromatics, and polymers productions.[2] Propylene is one of the most vital building blocks in the world petrochemical industry, where it finds applications in the production of propylene oxide, isopropanol, polypropylene and acrylonitrile.[3,4] Dehydrogenation is widely known as a highly endothermic process, which requires high temperatures (500 °C and above).[2,5] This kind of high reaction condition often promotes the production of undesired products via the cracking process, which ends up leading to the deactivation of the catalyst after being coked.

In the search for ways of alleviating this challenge that retards the life span of dehydrogenation catalysts, several research works have been carried out to get this problem addressed. For instance, Yan *et al.*[6] was able to employ the use of DFT calculation to study the effectiveness of the gallium oxide for the promotion of propane dehydrogenation. The study proposes a radical mechanism involved with the H abstraction from the propyl species, by Ga sites, and identified it as the rate-determining step. Besides, it was recognized that the propane dehydrogenation over Ga_2O_3(100) majorly takes the approach of direct dehydrogenation mechanism (DDH) and not the oxidative dehydrogenation (ODH) approach.

The study of Ming *et al.*[7] unveils that with the introduction of Sn on Pt catalyst, the alloyed surface was confirmed to have weakened the binding strength of propylene with the surface. The deductions made by Ming *et al.*[7] were found to be in line with Lauri and Karoliina[8] report, which indicated that alloying weakened the binding force of propylene and thereby prevent further dehydrogenation. This further increases the selectivity property of the catalyst[7]. Besides, Lauri and Karoliina's[8] study indicates that the low coking and high selectivity of Pt-Sn alloyed catalyst were due to the lack of active Pt step sites.

Further studies byTimothy[9] suggested that the introduction of Ga into the Pt surface has surface selectivity for olefins improved. It was also reported that PtGa exhibits better activity compared to PtSn alloyed surface.[9] Stephanie *et al.*[10] identified that the rise in hydrogen coverage reduces the binding force holding propylene to the Pt surface and increases the energy barriers towards the further dehydrogenation step. Oyegoke *et al.*[11] studies present that Cr was highly acidic and reactive, and the Cr site was confirmed to be active in the promotion of propane dehydrogenation. Furthermore, many other reports such as: Zhang *et al.*[12] studied V_2O_3; Eduard *et al.*[13] studied the palladium surface; Xie *et al.*[14] studied V_2O_3, etc., supported surface.

Theoretical studies in the literature have been concentrating mainly on the use of Pt catalyst with less attention for the appraisal of chromium oxide catalyst performance and how the catalyst can be improved. Hence, this analysis provides an insight into the thermodynamic and kinetic details of the reaction mechanism involved in the cracking of propane over a chromium oxide via combined use of the DFT and cluster approach. The deductions made from the results obtained

will allow a better understanding of how propane cracking can be inhibited when it is not desired in a reaction.

METHODOLOGY

Theoretical background

Computations were carried out with the use of the density functional theory (DFT) calculation method in the Spartan 18 software package. The calculations were run on an HP 15 Pavilion Notebook (Intel Core i3 Processor @ 1.8 GHz and 6 GB RAM).

The structures of reactant, catalyst, and different intermediate species were built and minimized via the use of the molecular mechanics (MMFF) method to remove strain energy. All the molecular mechanics optimized geometries were subjected to DFT calculation, and the B3LYP method was adopted, ensuring that the structures built do not show the presence of any negative imaginary frequency on the IR spectra result.

Literature confirms, 6-31G* and LANL2DZ basis set as one of the best sets for computations, when dealing with transition metals like chromium,[15] also more cost-effective computationally. Surveys reveal that the 6-31G* basis set is widely considered the best compromise in the terms of accuracy and speed and is the most frequently used basis set available for elements H–Kr. At the same time, heavy atoms are usually modeled *via* the use of the LANL2DZ basis set, which employs a capable core for all atoms larger than Ne[15].

The chromium (III) oxide catalyst cluster or slab used in this study was adopted from Brown *et al.*[16,] which was confirmed to be similar to the one used in the literature[17-19]. Research has shown that the IR spectrum of the cluster model obtained from a DFT study corresponds with the peaks obtained from the experimental analysis of chromium oxide IR spectrum. The study indicated that the cluster model is accurate and consistent.[16,18,20]

The properties of all concerned species were computed. This estimation was carried out via the use of the various statistical thermodynamic models and the use of output data obtained from density functional theory (DFT) computations carried out on Spartan 18. The DFT calculation presents input parameters such as the moment of inertia, total mass, and wavenumbers of the structures considered in this report, which were later used to calculate the free energies. The thermodynamic properties' model employed was adapted from the literature[21-23] and is presented in the Supplementary material to this paper. Besides, the chemical species' thermodynamic properties computations employed the use of the following conditions and models in the computation of Gibbs free energies:

a. Surface gas-phase species. The properties of gas-phase species were calculated accounting for all contributions such as translational, rotational, and vibrational motion effects to the overall species' free energies in the reaction steps:

$$G_{gas} = H_t + H_r + H_v + E_{elect} + ZPE - T(s_t + s_r + s_v) \quad (1)$$

b. Catalyst slab. In the case of the catalyst, all rotational and translation effects were assumed to be zero. This zero was due to the catalyst structure that was taken to be fixed (as a solid catalyst) in the estimation of the catalyst-free energies:

$$G_{cat} \approx E_{elect} + ZPE + H_v - T(s_v) \quad (2)$$

c. Species. The effect of vibrational motion was thoroughly taken. In contrast, two--thirds (2/3) translational and one half (1/2) rotational motion effects were considered in the calculation of free energies for the adsorbate (*i.e.*, the surface species) including the effect of surface configuration on the free energies:

$$G_{ads} = H_v + {}^2/_3H_t + ½H_r + E_{elect} + ZPE - T(s_v + {}^2/_3s_t + ½s_r + s_{config}) \quad (3)$$

An approximation model for 2D gas[24,25] was employed in the treatment of the adsorbate in studies as recommended by Campbell *et al.*,[24] where the adsorbate species account for the loss of a degree of freedom in both translational and rotation motion contributions, that is, hindered translator/hindered rotor approximation as an alternative harmonic oscillation approximation[26,27] which was reported to have underestimated the contribution of rotation and translational motion or effect in the computation of total free energies for adsorbates.

Reaction mechanism scheme

Here, the cracking of the propane was considered to be initiated with the physisorption of propane on the catalyst surface. Followed by the activation of the C–H bond in the propane on the catalyst (*i.e.*, assessing the effect across alpha-carbon and surface sites like Cr–Cr and Cr–O), along with the activation of propane across the C–H bond to give isopropyl (1-propyl or 2-propyl). After this, next step tends to evaluate the chance of the C–C bond scission of the adsorbed species of isopropyl. This study involves the thermodynamic feasibility of the different surface sites such as Cr–Cr, and Cr–O, leading to the production of adsorbed ethyl and methyl. Next was the association of H with methyl species, the further scission of C–H bond in methyl and ethyl species, to give adsorbed methyl (CH_3), methylene (CH_2) and ethylene (C_2H_4). They were evaluated as across different sets of surface sites aforementioned. It is diagrammatically presented in Fig. 1.

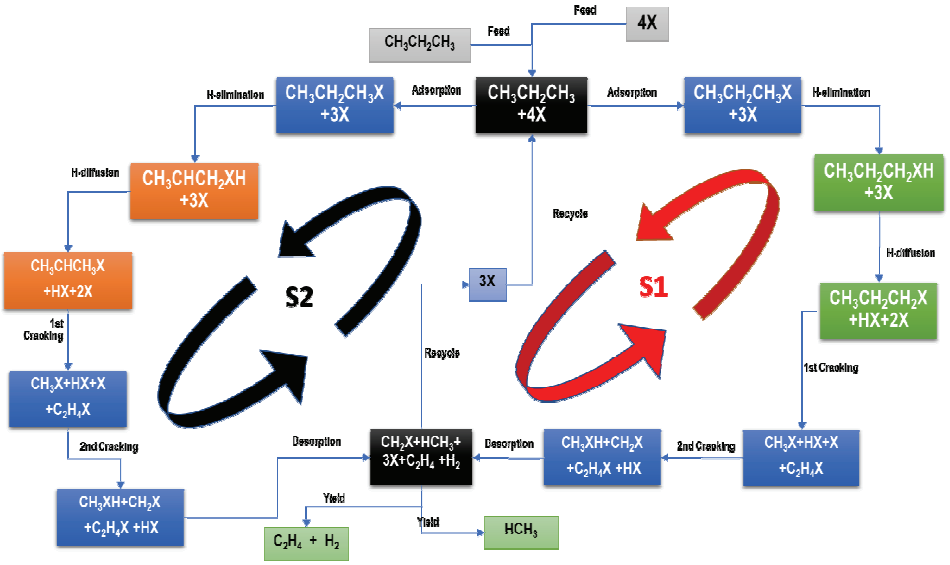

Fig. 1. A representation of the reaction routes studied.

The propane cracking mechanism is presented with the use of chemical equations, where sets of chemical reaction equations (reaction scheme) are employed to display the elementary reaction steps involved in the process in this study.

Propane activated at alpha-carbon (S1):

$$C_3H_8 + X \leftrightarrow CH_3CH_2CH_3X \quad (4)$$

$$CH_3CH_2CH_3X + X \leftrightarrow CH_3CH_2CH_2XH \quad (5)$$
$$CH_3CH_2CH_2XH + X \leftrightarrow CH_3CH_2CH_2X + HX \quad (6)$$
$$CH_3CH_2CH_2X + X \leftrightarrow CH_3X + CH_2CH_2X \quad (7)$$
$$CH_3X + HX \leftrightarrow CH_3XH + X \quad (8a)$$
$$CH_3X + X \leftrightarrow CH_2X + HX \quad (8b)$$
$$CH_3XH \leftrightarrow HCH_3 + X \quad (9a)$$
$$2HX \leftrightarrow H_2 + 2X \quad (9b)$$
$$CH_2CH_2X \leftrightarrow CH_2CH_2 + X \quad (9c)$$

Propane activated at beta-carbon (S2):

$$C_3H_8 + X \leftrightarrow CH_3CH_2CH_3X \quad (10)$$
$$CH_3CH_2CH_3X + X \leftrightarrow CH_3CHCH_3XH \quad (11)$$
$$CH_3CHCH_3XH + X \leftrightarrow CH_3CHCH_3X + HX \quad (12)$$
$$CH_3CHCH_3X + X \leftrightarrow CH_3X + CH_2CH_2X \quad (13)$$
$$CH_3X + HX \leftrightarrow CH_3XH + X \quad (14a)$$
$$CH_3X + X \leftrightarrow CH_2X + HX \quad (14b)$$
$$CH_3XH \leftrightarrow HCH_3 + X \quad (15a)$$
$$2HX \leftrightarrow H_2 + 2X \quad (15b)$$
$$CH_2CH_2X \leftrightarrow CH_2CH_2 + X \quad (15c)$$

It was noted that the isopropyl(s), *i.e.*, 1-propyl activated at the alpha-carbon (S1) or 2-propyl activated at the beta-carbon (S2), that propane can be activated in either ways. This study tries to identify the thermodynamically feasible path that best promotes propane cracking and to identify its potential rate-determining step across the chromium (III) oxide surface. The X represents catalyst surface sites, which could be chromium (Cr) or oxygen (O) sites.

RESULTS AND DISCUSSIONS

Findings from the study of the mechanism involved in the cracking of propane into small hydrocarbon over the chromium oxide catalyst are discussed here. The results obtained for the assessment of different surface sites (such as Cr–Cr and Cr–O), and the point of propane activation (at alpha and beta carbon) were evaluated. The set of results for the reaction energies, energy barrier, including the reaction profiles, was presented in different forms for the provision on insight on the feasible reaction path and the rate-determining step involved in the cracking of the propane.

In Figs. 1–4, the Cr–Cr and Cr–O denote sets of different catalyst surface sites while S1 and S2 imply activation at alpha-carbon and beta-carbon, respectively. The R depicts the reverse reaction while F represents forward reaction. Besides, ‘ads,’ ‘suf1’, ‘diff,’ ‘cra1’, ‘cra2’ and ‘des’ represent the six elementary reaction steps involved in the study, that is, adsorption, first abstraction, diffusion, cracking/scission, further scission of adsorbed species, and desorption respectively.

Reaction energies of the elementary reaction steps

All chemical processes or reactions involve energy changes. In some reactions, these energy changes could either be an increase or a decrease in the system's overall energy. In another reaction, we see it as a change in the temperature. In other reactions, this change is observed when a reaction starts to give off light or when a reaction begins with a presence of light. By the physical law (that is, the law of conservation of energy), it is well known that the total system energy must remain unchanged. Usually, a chemical reaction will release or absorb in the form of light, heat, or both.

Here, the results of the reaction energies are presented, displaying the quantity of energy lost or gained as the reaction proceeds in terms of increase and decrease. Figs. 1 and 2 present the sets of reactions energy collected for the elementary reaction making up the process. This energy lost or gain was obtained via use of the difference in the amounts of stored chemical energy between the products and the reactants for both forward and backward reactions.

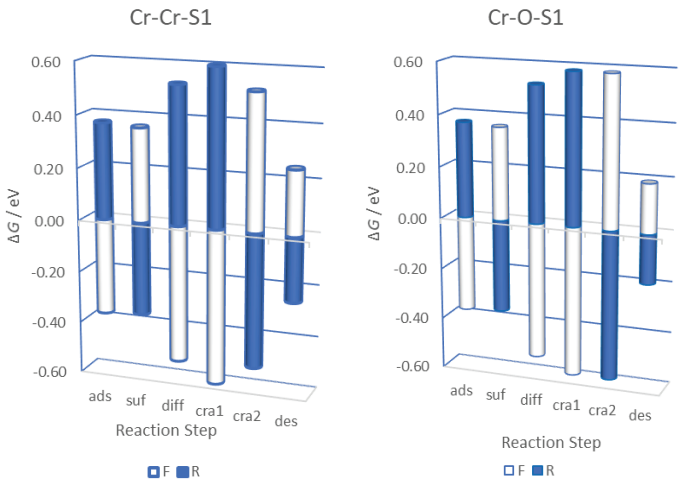

Fig. 2. Reaction energy, Δ*G* / eV, for the reaction path across: a) Cr–Cr and b) Cr–O sites activated at the alpha-carbon (S1) atom of the propane.

The study of the results presented for the forward (F) reactions in Fig. 2a for the propane cracking across Cr–Cr surface sites activated at alpha carbon (S1) indicated that propane adsorption (ads), H abstraction (suf), H diffusion (diff), cracking of isopropyl (cra1), second cracking (cra2) and desorption (des) steps displayed –0.37, 0.36, –0.53, –0.60, 0.52 and 0.25 eV, respectively. The results show that propane adsorption (ads), H diffusion (diff), and cracking of isopropyl (cra1) steps displayed negative reaction energies, which implies that they are exothermic steps. Whereas H abstraction (suf), second cracking (cra2), and des-

orption (des) steps displayed positive reaction energies, which indicated that they are endothermic steps.

The reaction energies of the elementary steps evaluated for Cr–O sites activated at alpha carbon (S1) displayed –0.37, 0.36, –0.53, –0.58, 0.58 and 0.19 eV for the forward (F, *i.e.*, while bars in Fig. 2b) reaction for propane adsorption (ads), H abstraction (suf), H diffusion (diff), cracking of isopropyl (cra1), second cracking (cra2) and desorption (des) steps respectively. Fig. 2b displays the results obtained for the evaluation of propane cracking across the Cr–O sites. The results displayed similar kind of negative reaction energies for the propane adsorption (ads), H diffusion (diff), and cracking of isopropyl (cra1) steps indicating that they are exothermic steps as well. Just as it was observed for the H abstraction (suf), second cracking (cra2) and desorption (des) step that showed positive reaction energy, which suggested that they are endothermic steps as well.

For propane activated at beta carbon (S2), studies across the Cr-Cr sites present the reaction energies of the elementary steps as -0.37, 0.26, -0.45, -0.58, 0.52 and 0.25 eV while Cr–O presents its reaction energies for its elementary reaction steps as -0.37, 0.34, -0.48, -0.61, 0.58 and 0.19 eV for the forward (F *i.e.* white bars in Fig. 3) reaction for propane adsorption (ads), H abstraction (suf), H diffusion (diff), cracking of isopropyl (cra1), second cracking (cra2) and desorption (des) steps respectively.

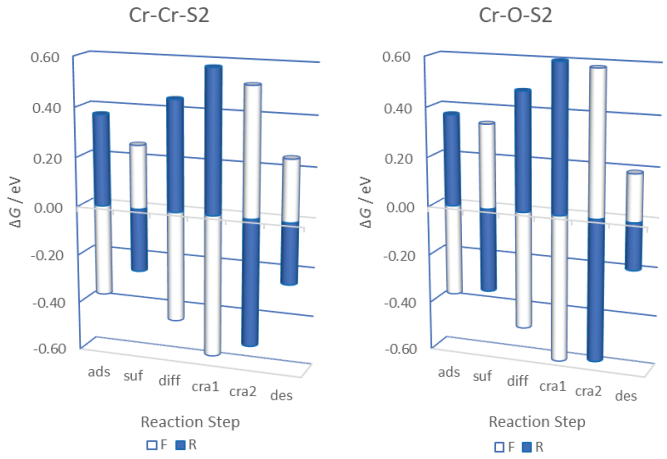

Fig. 3. Reaction energy, Δ*G* / eV, for the reaction path across: a) Cr–Cr and b) Cr–O sites activated at the beta-carbon (S2) atom of the propane.

Fig. 3 displays the results obtained in the evaluation of propane cracking across the Cr–Cr and Cr–O sites. The results displayed similar kind of negative reaction energies for the propane adsorption (ads), H diffusion (diff) and cracking of isopropyl (cra1) steps indicating that they are exothermic steps as well. Also, it

was observed that the H abstraction (suf), second cracking (cra2), and desorption (des) steps exhibited positive reaction energy, which suggested that they are endothermic steps.

The results obtained for H abstraction (suf) presented in Fig. 3 indicated that the reaction energy for Cr–Cr sites was lower when compared with that of the Cr–O sites. For H diffusion and first cracking step, the reaction energy for the Cr–Cr site was found to be less negative compared to Cr–O sites. The second cracking and desorption step showed that the reaction energy of the Cr–Cr site is much lower compared to Cr–O sites except for the desorption step, which was the reverse.

The assessment of the reaction energies across the different surface sites (depicting different reaction routes) indicated that all the propane adsorption (ads), H diffusion (diff), and cracking of isopropyl (cra1) steps are exothermic steps while the H abstraction (suf), second cracking (cra2) and desorption (des) steps were found to be endothermic steps.

The energy barrier of the elementary reaction steps

The results collected for this study are diagrammatically represented in Figs. 4 and 5. These figures display the results for the Cr–Cr and Cr–O sites, which indicate the different energy barriers for the different reaction steps in the cracking/scission of propane.

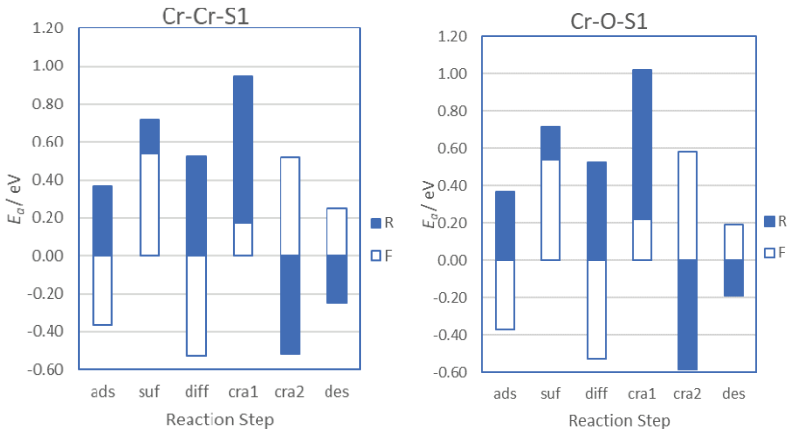

Fig. 4. Energy barrier, E_a / eV, for the surface reaction steps across: a) Cr–Cr and b) Cr–O sites activated at the alpha-carbon (S1) atom of the propane.

Fig. 4 shows that all the reaction steps involved in the propane adsorption (ads), and hydrogen diffusion (diff) indicated a negative energy barrier. The findings imply that they are barrierless steps, unlike the other steps like hydrogen abstraction (suf), first cracking (cra1), second cracking (cra2) and desorption (des) steps, which showed a positive activation energy (or energy barrier).

Further evaluation of the energy barriers across the Cr–Cr and Cr–O for the S1 route indicated that similar kind of energy barriers were displayed for adsorption (ads, *i.e.*, –0.37 eV), H abstraction (suf, *i.e.*, 0.54 eV), and H diffusion (diff, *i.e.*, 0.53 eV) but varying energy barriers for other steps. Nevertheless, the other steps, the 1st cracking (cra1) step for Cr–Cr site (0.17 eV) were found to show a lower energy barrier compared Cr–O (0.22 eV) while for the second cracking (cra2) and desorption (des) step, Cr–Cr site (0.52 and 0.25 eV) energy barrier was found to be higher than for the Cr–O sites (0.58 and 0.19 eV).

The assessment of the results presented for the energy barriers across the Cr–Cr and Cr–O sites in the route of S1 (that is, the path that activate propane at the beta-carbon atom) revealed that the energy barriers displayed for adsorption (ads), H abstraction (suf), H diffusion (diff), 1st cracking (cra1), 2nd cracking (cra2) and desorption (des) step are –0.37, 0.54, –0.53, 0.17, 0.52 and 0.25 eV, and –0.37, 0.54, –0.53, 0.22, 0.58 and 0.19 eV, respectively, for the sites.

The results in Fig. 5 show that both the propane adsorption (ads), and H diffusion (diff) steps displayed a negative energy barrier for their forward reactions. The results imply that the steps are barrierless. In contrast, the other steps like hydrogen abstraction (suf), first cracking (cra1), second cracking (cra2), and desorption (des) steps showed a positive activation energy (or energy barrier), which indicated that they would demand energy for these steps to proceeds.

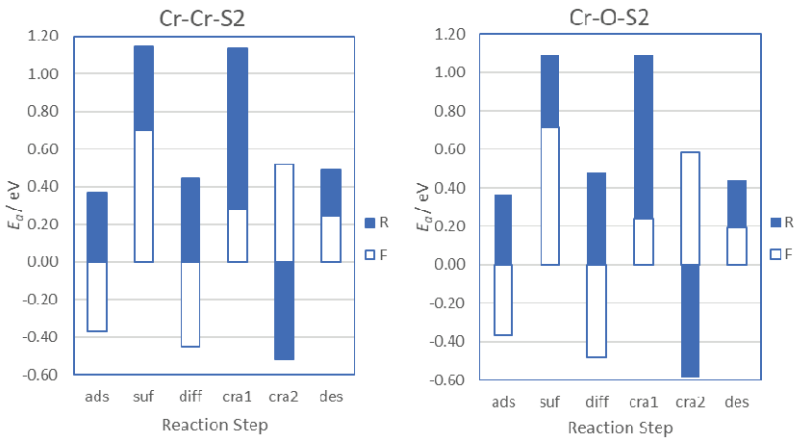

Fig. 5. Energy barriers, E_a / eV, for the surface reaction steps across: a) Cr–Cr and b) Cr–O path sites activated at the beta-carbon (S2) atom of the propane.

The evaluation of the entire energy barriers in the Cr-Cr (S1), Cr-O (S1), Cr–Cr (S2) and Cr–O (S2) reaction routes indicate that H abstraction (*i.e.*, propane activation to give isopropyl) shows the highest energy barrier followed by the 2nd cracking step. Across the S1 route, Cr–Cr sites displayed the lowest barrier (0.17 eV) for the first cracking step (cracking initiation) that promotes crack-

ing while Cr–O shows a higher barrier (0.22 eV) in Fig. 4. For the S2 route, the Cr-Cr sites displayed a higher barrier of 0.28 eV, while the Cr–O site displayed 0.24 eV in Fig. 5. This implies that across all reaction's routes, the Cr–Cr sites in the S1 route showed the lowest barrier (that will require the least energy) for the cracking to get initiated. The reaction routes along the path of the S1 scheme indicated that the path which interacted through the Cr–Cr sites would be thermodynamically feasible.

The findings indicate that the activity of Cr–Cr along the route of the S1 scheme will tend to promote propane cracking due to its lower energy barrier in its routes. It could also imply that surface with more Cr sites will better crack propane. Furthermore, it indicates that the Cr site remains an active component in the cracking of propane. That is why the surface dominated with Cr sites tends to promote deep dehydrogenation or cracking, which has been traced to the activity of the site. These findings were found to agree with the report of Jibril,[28] which indicates that the activeness of the Cr site greatly influences the dehydrogenation of propane into propylene.

Evaluation of thermodynamic feasibility of a different reaction route or path and the identification of potential rate-limiting steps in the cracking process

The assessment of the six elementary steps, involved in the cracking of propane across the Cr–Cr and Cr–O sites on the route of S1, indicate that the propane adsorption (ads), H abstraction (suf), H diffusion (diff), and second cracking steps displayed a similar trend.

However, it was observed that the 1st cracking step displayed a lower barrier for the Cr–Cr site, while a higher barrier was identified for the Cr–O. Similarly, a lower barrier was recorded for the Cr–Cr site while a higher barrier was displayed for the Cr–O site for both 2nd cracking and desorption steps. The findings are evident in Fig. 6, which displayed the profiles for the different reaction routes. The reaction routes along the path of the S1 scheme indicated that the path which interacted through the Cr–Cr sites would be thermodynamically feasible.

The study of propane cracking along the route of S2 indicated that participation of the Cr–Cr site displayed lower energy profiles in all steps of the reaction. It is graphically displayed in Fig. 7. The findings obtained from the results presented the reaction profiles in Fig. 7 indicated that the Cr–Cr sites would be more thermodynamically feasible when compared to Cr–O site in the assessment of scheme S2 routes due to its lower energy barriers displayed.

In general, it was primarily found that most of the surface species adsorbed on Cr–Cr sites displayed negative energy compared to those adsorbed on Cr–O sites, which is evident in Figs. 6 and 7. The findings, however, imply that species tend to be more stable on the Cr–Cr site than on the Cr–O sites. In other words, it can be said that the binding force holding the species to the Cr–Cr sites is

stronger than on the species adsorbed across the Cr–O sites. This force has made desorption energy barrier to be lower for Cr–O sites when compared to Cr–Cr sites. This strong force on the Cr–Cr sites, thereby promotes further cracking, which end-up leading to the coking of the sites.

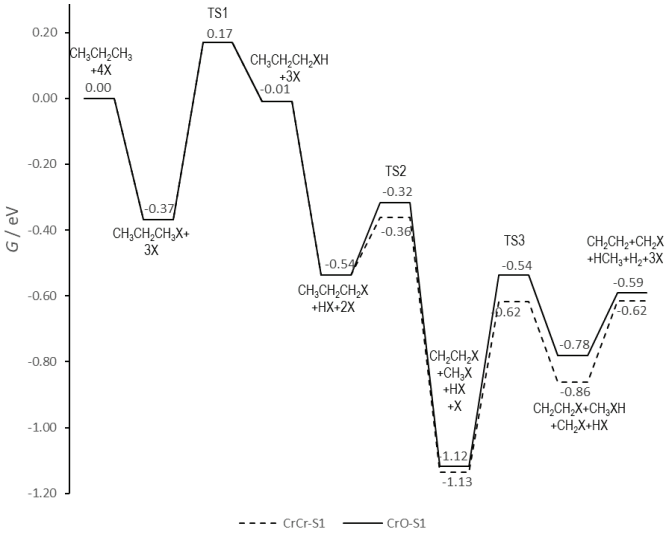

Fig. 6. Propane cracking reaction path across Cr–Cr (broken lines) and Cr–O (continuous line) sites using the reaction scheme S1.

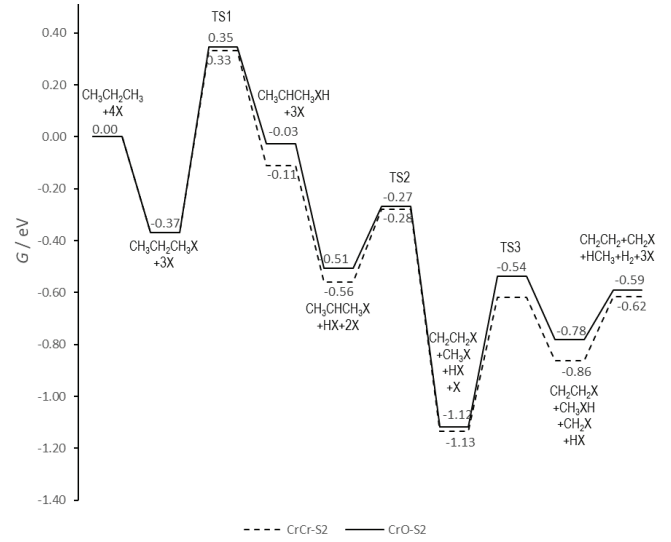

Fig. 7. Propane cracking reaction path across Cr–Cr (broken lines) and Cr–O (continuous line) sites using the reaction scheme S2.

As a way of preventing cracking or coking during H abstraction processes when cracking of the molecules or species is not desired, this study suggests, Cr site substitution, as a way to aid in alleviating the production of undesired products such as coke, methylene (CH_2), methyl (CH_3) and ethyl (C_2H_5) during the use of chromium oxide catalyst. Another way of preventing the cracking when it is not desired, Stephanie *et al.*[10] in their studies identified the co-feeding of propane with hydrogen, which will primarily prevent cracking.

Therefore, the most thermodynamically favored reaction pathway, for the cracking or scission of propane into small hydrocarbons on chromium oxide, would be Cr–Cr (S1) as it was found to have the lowest energy barrier for the H abstraction and also showed a lower energy barrier for the cracking initiation step. These findings indicate that Cr–Cr (S1) will effectively promote the cracking of propane. The H abstraction step (where C–H bond activation of propane at the alpha (or terminal) carbon takes place on Cr site) would be the potential rate-determining step (RDS) due to its significant energy barrier displayed in its profile for Cr–O (S1) in Fig. 4. This finding showed a similar RDS to that of Yu-Jue *et al.*,[29] which confirms the first C–H activation step (*i.e.*, first abstraction step) as its RDS for propane dehydrogenated on vanadium oxide. However, the 1st cracking step's lower energy barrier enables cracking to hold with less energy demand along such a reaction route.

CONCLUSIONS

The investigation into the cracking of propane to small hydrocarbon on a chromium oxide catalyst via the use of a DFT study approach was carried out. The study was done in order to understand the reaction routes that promote the production of products like coke, methylene (CH_2), methyl (CH_3), ethyl (C_2H_5) and many others when such kind of products are not desired.

The study identified that the reaction route where propane gets activated at the alpha-carbon (S1) across the Cr–Cr sites, as the most thermodynamically feasible reaction route, which would be the best at promoting the production of cracked products. Moreover, the H abstraction (*i.e.*, C–H bond activation) was found to be RDS along that reaction route. It was also identified that the strong force that binds species strongly to Cr sites aid in promoting the cracking of the species.

The understanding gained from this investigation reveals the reaction path that has to be inhibited the production of propylene, BTX and many others where crack species/products are not desired. It is therefore recommended that the dormancy of Cr sites across the surface of the catalyst could be reduced *via* the use of oxygen/oxidants or substitution of some Cr sites with metals that would best promote the desired products.

NOMENCLATURE

F	Forward reaction	E_a	Activation energy or energy barrier
R	Reverse reaction	E_{elect}	Electronic energy
ads	Adsorption step	S_{config}	Configurational entropy
suf	H abstraction	ZPE	Zero-point energy
diff	H diffusion	T	Temperature
cra1	1st cracking step	$\nu_{n,i}$ or ν_i	Wavenumbers of species
cra2	2nd cracking step	k_g	Boltzmann constant
des	Desorption step	h	Planck constant
vib.	Vibration effect/contribution	m	Mass of specie
transl	Translation effect/contribution	P_0	Standard pressure
rot	Rotation effect/contribution	$I_{r,linear}$, I_a, I_b, I_c	Moment of inertia
R	Gas constant	ρ_r	Symmetry number of the species
ΔG	Reaction energy	^{o}	Standard state
G	Gibbs energy		
H_i	Enthalpy (where i is either vib (v), transl (t) or rot (r))		
s_i	Entropy (where i is either vib (v), transl (t) or rot (r))		

SUPPLEMENTARY MATERIAL

The additional data are available electronically at the pages of journal website: http://www.shd.org.rs/JSCS/, or from the corresponding author on request.

Acknowledgement. The first author wishes to acknowledge the support of the Petroleum Technology Development Fund Abuja, Nigeria, for funding his program.

И З В О Д

ИЗРАЧУНАВАЊЕ ТЕОРИЈОМ ФУНКЦИОНАЛА ГУСТИНЕ МЕХАНИЗМА КРЕКОВАЊА ПРОПАНА НА ХРОМ (III)–ОКСИДУ КЛАСТЕРСКИМ ПРИСТУПОМ

TOYESE OYEGOKE[1,2], FADIMATU NYAKO DABAI[1], ADAMU UZAIRU[3] и BABA EL-YAKUBU JIBRIL[1]

[1]Chemical Engineering Department, Faculty of Engineering, ABU Zaria, Nigeria, [2]Laboratoire de Chimie, ENS Lyon, l'Universite de Lyon, 69007, Lyon, France u [3]Chemistry Department, Faculty of Physical Sciences, ABU Zaria, Nigeria

Таложење кокса на катализатору и производња нежељених производа током трансформисања пропана у пропилен представља велики изазов наменском приступу производње пропилена. Механизам који доприноси решавању овог проблема је теоријски проучаван преко реакционих путева крековања. Спроведена студија користи DFT и кластерски приступ, да би се разумеле реакције које доприносе коксовању катализатора, као и у потрази за кинетичким и термодинамичким подацима реакционог механизма који је присутан у процесима на Cr_2O_3. Идентификовани су ступањ који одређује брзину реакције (RDS) и могући путеви који лако промовишу производњу малих угљоводоника као што су етилен, метан и многи други. Студија сугерише, супституцију Cr-места или додавање кисеоника, као начин да се помогне спречавање дубоке дехидрогенизације код конверзије пропана у пропилен. Ова информација ће помоћи да се побољша перформанса Cr_2O_3 катализатора и даље побољша принос производа.

(Примљено 21. маја, ревидирано 18. јула, прихваћено 20. јула 2020)

REFERENCES

1. S. Asadi, L. Vafi, R. Karimzadeh, *Micropor. Mesopor. Mat.* **255** (2018) 253 (https://dx.doi.org/10.1016/j.micromeso.2017.07.018)
2. H. A. Wittcoff, B. G. Reuben, J. S. Plotkin, *Industrial Organic Chemicals*, John Wiley & Sons, Hoboken, FL, 2000, p. 211 (https://dx.doi.org/10.1002/0471651540)
3. S. Budavari, *Propylene - The Merck Index*, Merck & Co., Kenilworth, NJ, 1996, p. 1
4. Y. Ren, F. Zhang, W. Hua, Y. Yue, Z. Gao, *Catal. Today* **148** (2009) 3 (https://dx.doi.org/10.1016/j.micromeso.2017.07.018)
5. J. C. Philip, *Survey of Industrial Chemistry*, Springer, Berlin, 2001, p. 2
6. L. Yan, Z. H. Li, J. Lu, K. N. Fan, *J. Phys. Chem., C* **112** (2008) 51 (https://dx.doi.org/10.1021/jp807864z)
7. Y. Ming-Lei, Y. A. Zhu, X. G. Zhou, Z. J. Sui, D. Chen, *ACS Catal.* **2** (2012) 1247 (https://dx.doi.org/10.1021/cs300031d)
8. N. Lauri, H. Karoliina, *ACS Catal.* **3** (2013) 3026 (https://dx.doi.org/10.1021/cs400566y)
9. H. Timothy, *Computational study of the catalytic dehydrogenation of propane on Pt and Pt3Ga catalyst*, Ghent University, Ghent, 2015, p. 15
10. S. Saerens, M. K. Sabbe, V. V. Galvita, E. A. Redekop, M.-F. Reyniers, G. B. Marin, *ACS Catal*. **7** (2017) 7495 (https://dx.doi.org/10.1021/acscatal.7b01584)
11. T. Oyegoke, F. N. Dabai, A. Uzairu, B. Jibril, *B. J. Pure Appl. Sci.* **11** (2018) 178 (https://dx.doi.org/10.4314/bajopas.v11i1.29S)
12. J. Zhang, Z. R-Jia, C. Q-Yu, S. Z-Jun, Z. X-Gui, Z. Y-An, *Cat. Today* (2020), in press (https://dx.doi.org/10.1016/j.cattod.2020.02.023)
13. E. Araujo-Lopez, L. Joos, B. D. Vandegehuchte, D. I. Sharapa, F. Studt, *The J. of Phys. Chem. C* **124** (2020) 3171 (https://dx.doi.org/10.1021/acs.jpcc.9b11424)
14. Y. Xie, R. Luo, G. Sun, S. Chen, Z. J. Zhao, R. Mu, *RSC Chem. Sci.* **11** (2020) 3845 (https://dx.doi.org/10.1039/C8CY00564H)
15. J. H. Warren, *A guide to molecular mechanics and quantum chemical calculations*, Wavefunction, Irvine, CA, 2003, p. 89
16. P. Brown, J. Forsyth, E. Lelievre-Berna, F. Tasset, *J. Phys.: Condens. Matter* **14** (2002) 1957 (https://dx.doi.org/10.1088/0953-8984/14/8/323)
17. W. Yanbiao, G. Xinxin, W. Jinla, *Phys. Chem. Chem. Phys.* **12** (2010) 2471 (https://dx.doi.org/10.1039/B920033A)
18. C. Compere, D. Costa, L. Jolly, E. Mauger, C. Gessner–Prettre, *New J. Chem.* **24** (2000) 993 (https://dx.doi.org/10.1039/B005313I)
19. S. Veliah, K. Xiang, R. Pandey, J. Recio, J. Newsam, *J. Phys. Chem., B* **102** (1997) 1126 (https://dx.doi.org/10.1021/jp972546m)
20. T. Oyegoke, F. N. Dabai, A. Uzairu, B. Y. Jibril, *Eur. J. Mat. Sci. Eng*. **5** (2020) 173 (https://dx.doi.org/10.36868/ejmse.2020.05.04.173)
21. N. M. Laurendeau, *Statistical Thermodynamics: Fundamentals and Applications*, Cambridge University Press, Cambridge, 2005
22. I. Kennedy, H. Geering, M. Rose, A. Crossan, *Entropy* **21** (2019) 454 (https://dx.doi.org/10.3390/e21050454)
23. T. L. Hill, *An Introduction to Statistical Thermodynamics,* Dover Publications Inc., New York, 1960
24. C. T. Campbell, L. H. Sprowl, L. Árnadóttir, *J. Phys. Chem.* **120** (2016) 10283 (https://dx.doi.org/10.1021/acs.jpcc.6b00975)
25. A. Savara, *J. Phys. Chem., C* **117** (2013) 15710 (https://dx.doi.org/10.1021/jp404398z)

26. L. H. Sprowl, C. T. Campbell, L. Arnadottir, *J. Phys. Chem., C* **121** (2017) 17 (https://dx.doi.org/10.1021/acs.jpcc.7b03318)
27. L. H. Sprowl, C. T. Campbell, L. Arnadottir, *J. Phys. Chem., C* **120** (2016) 9719 (https://dx.doi.org/10.1021/acs.jpcc.5b11616)
28. B. Y. Jibril, *Appl. Catal., A* **264** (2004) 193 (https://dx.doi.org/10.1021/ie000285o)
29. D. Yu-Jue, Z. H. Li, K. N. Fan, *J. Mol. Catal., A* **379** (2013) 122 (https://dx.doi.org/10.1016/j.molcata.2013.08.011)
30. P. Wang, S. N. Steinmann, G. Fu, C. Michel, P. Sautet *ACS Catal.* **7** (2017) 1955 (https://dx.doi.org/10.1021/acscatal.6b03544)
31. F. Maldonado, A. Stashans, *Surface Rev. Lett.* **23** (2016) 1650037 (https://dx.doi.org/10.1142/S0218625X16500372)
32. Z. J. Zhao, T. Wu, C. Xiong, G. Sun, R. Mu, L. Zeng, J. Gong, *Angew. Chem. Int. Ed.* **57** (2018) 6791 (https://dx.doi.org/10.1002/anie.201800123).